Published in final edited form as:
J Agric Food Chem. 2011 May 11; 59(9): 4979–4986. doi:10.1021/jf104901g.

Resveratrol Metabolites Do Not Elicit Early Pro-apoptotic Mechanisms in Neuroblastoma Cells

Jason D. Kenealey, **Lalita Subramanian**, **Paul R. Van Ginkel**, **Soesiawati Darjatmoko**, **Mary J. Lindstrom**, **Veronika Somoza**, **Sunil K. Ghosh**, **Zhenlei Song**, **Richard P. Hsung**, **Glen S. Kwon**, **Kevin W. Eliceiri**, **Daniel M. Albert**, and **Arthur S. Polans***
Departments of Biomolecular Chemistry, 1300 University Avenue, Room 587 Medical Science Center, Madison, WI 53705 (JDK, ASP), Ophthalmology and Visual Sciences, 2828 Marshall Court, Suite 200, Madison, WI 53705 (LS, PRvG, SD, DMA, ASP), and Biostatistics and Medical Informatics, K6/446 Clinical Sciences Center 600 Highland Avenue, Madison, WI 53792 (MJL), School of Medicine and Public Health; Institute of Nutritional and Physiological Chemistry, Althanstrasse 14 (UZA II), University of Vienna (VS); Pharmaceutical Sciences Division, School of Pharmacy, 777 Highland Avenue, Madison, WI 53705 (SKG, ZS, RPH, GSK); Laboratory for Optical and Computational Instrumentation (KWE), College of Engineering, 1415 Engineering Drive, Madison, WI 53706 University of Wisconsin, Madison

Abstract

Resveratrol, a non-toxic polyphenol, has been shown to inhibit tumor growth in a xenograft mouse model of neuroblasoma. However, resveratrol is rapidly metabolized, mainly to its glucuronidated and sulfated derivatives. In this study we demonstrate that resveratrol alone, and not the glucuronidated or sulfated metabolites, is taken up into tumor cells, induces a rise in $[Ca^{2+}]_i$, and ultimately leads to a decrease in tumor cell viability. A new water-soluble resveratrol formulation was delivered directly at the site of the tumor in a neuroblastoma mouse model. The amount of unmodified resveratrol associated with the tumor increased more than 1000-fold. The increase of unmodified resveratrol associated with the tumor resulted in tumor regression. The number of residual tumor cells that remained viable also decreased as the ratio of the metabolites relative to unmodified resveratrol declined.

Keywords

Resveratrol; Neuroblastoma; Calcium Signaling; Bioaviailability

Introduction

Over the past several decades researchers have focused on finding drugs that specifically affect cancer cells without harming normal cells. Often this research has focused on naturally occurring compounds. Jang et al. (1) found that resveratrol (Res), a natural product found in grapes, peanuts, and Japanese knotweed, could prevent cancer in a mouse model of melanoma. Following this initial study the anti-cancer effect of Res has been studied in a variety of cancers. In this study we focus on neuroblastoma, a childhood cancer that most often arises in the sympathetic nerves of the adrenal gland and accounts for 15% of the childhood deaths from cancer (2, 3). Despite aggressive combination therapeutic

Arthur S. Polans, Ph.D., M.D. Matthews Retina Research Foundation Professor, Department of Ophthalmology and Visual Sciences, Rm K6/466 Clinical Sciences Center, 600 Highland Avenue, University of Wisconsin, Madison, WI 53792, 608-265-4423 (phone), 608-265-6021 (fax), aspolans@wisc.edu.

approaches, more than 60% of the children with high-risk neuroblastoma do not survive due to metastasis, high recurrence and chemo-resistance. Between 20% and 50% of high-risk cases do not respond adequately to induction high-dose chemotherapy and are progressive or refractory. Relapse after completion of frontline therapy is also common. Further, the quality of life of these children is threatened by therapy-induced toxicity (4). Thus, these children would benefit from a non-toxic compound, such as resveratrol, to alleviate the devastating side effects of standard therapeutics.

In vitro mechanistic studies have indicated that Res can activate pathways implicated in apoptosis (5). However, in mouse xenograft models where Res has been shown to inhibit tumor growth when delivered orally there is little evidence of apoptosis. One possible explanation for the absence of apoptosis in these mouse models is the low bioavailability of Res. The inhibition of tumor growth achieved at lower levels of resveratrol could be explained by other mechanisms of action, including anti-proliferative and anti-angiogenic activities (6).

In vivo studies in animals and humans indicate that resveratrol is poorly absorbed from the gastrointestinal tract and undergoes extensive first-pass metabolism, mainly glucuronidation and sulfation, in the gut and liver leading to trace amounts of the compound in the serum. The resveratrol metabolites are then dependent on ABC transporters for uptake (7-10). Our previous studies in neuroblastoma indicate that despite low bioavailability, resveratrol is effective at inhibiting tumor growth when delivered orally (5). Indeed, when the serum levels of Res were measured in such rodent studies there was less than 1 μM of Res and twenty fold higher levels of the Res metabolites within half an hour of drug delivery.

The anti-cancer properties of Res could result either from activation of pathways through extra-cellular receptors, or uptake into cells and activation of intra-cellular regulators. Currently, the only evidence for entry of Res into cells comes from cell types that have specialized uptake mechanisms (11). Determining the subcellular localization of Res would help elucidate potential binding partners and mechanisms whereby Res induces tumor cell death. We therefore want to investigate how Res and its metabolites might differ in cellular uptake, pathway activation, and ultimately in tumor cell death. An early pathway activated by Res, in tumor cells, is calcium signaling by increasing cytoplasmic calcium (12). Calcium signaling plays a vital role in cell proliferation, angiogenesis and cell death (13). The versatility of calcium signaling is due to the cell's ability to control the localization and concentration of the signal, and the array of responsive calcium binding proteins in the cell. A sustained increase in $[Ca^{2+}]_i$, in tumor cells is thereby associated with the activation of pathways leading to inhibition of tumor cell proliferation as well as cell death (14). Previous studies (15, 16) have shown that chelating $[Ca^{2+}]_i$ with BAPTA-AM inhibits the Res-induced tumor cell death.

In this study we demonstrate that Res enters neuroblastoma cells, induces a calcium signal and ultimately decreases tumor cell viability. Both Res uptake and ER calcium release occur within minutes of drug exposure. Meanwhile, we present evidence using purified derivatives that Res's sulfated and glucuronidated metabolites are not taken up by neuroblastoma cells and, therefore, are incapable of activating calcium signals. Consequently, the Res metabolites have no impact on the viability of these cells. Therefore metabolism diminishes Res's anti-cancer effects. As proof of principle, we demonstrate a method of Res delivery that reduces its rapid metabolism to achieve apoptosis and tumor regression in a neuroblastoma mouse model.

Methods

Materials

Purified resveratrol was purchased from Cayman Chemical (Michigan, USA). Fura-2 was purchased from Molecular Probes. Pluronic® P104 was kindly donated by BASF (BASF, Mount Olive, NJ, USA). All other chemicals were of reagent grade. Athymic nu/nu mice were purchased from Harlan Sprague Dawley Inc. (Indianapolis, USA). Animals were housed in a pathogen-free isolation facility. All animal care and treatment protocols were in compliance with the guidelines and approved by the University of Wisconsin- Madison Animal Care and Use Committee.

Cell culture

SK-N-AS and NGP neuroblastoma cell lines were grown as adherent cells at 37°C, 5% CO_2 in RPMI 1640 supplemented with 10% (v/v) fetal bovine serum (Atlanta Biologicals, Lawrenceville, GA, USA), 10 mmol/L HEPES, and 1% penicillin-streptomycin-amphotericin B (Sigma, St. Louis, MO, USA).

Res formulation containing P104 (R-P104)

200μl ethanol (2%) was added to 20mg Res, then dissolved in 10mL of a 10% P104 aqueous solution, and filtered through a 0.2μm syringe filter to obtain a clear pale yellow solution. The concentration of Res in the solution was quantified by HPLC prior to use (see below).

In vitro cell viability

Cells were grown in 96-well microtiter plates for 2 days. Drug treatments were started and corresponding treatment media were replenished after two days. 4 days later Cell Titer Blue reagent was added according to the manufacturer's instructions (Promega, Madison, WI, USA). Fluorescence was measured at excitation/emission wavelengths of 560/590 nm, using a fluorescence plate reader (Molecular Devices, Sunnyvale, CA, USA).

Calcium Imaging

Cells were imaged following a standard protocol (12). Briefly, neuroblastoma cells were loaded with fura-2-AM for 30 minutes at 37°C followed by a 30 minute incubation at room temperature. Cells were subsequently imaged on the BD Pathway microscope. The fura-2 loaded cells were alternately excited at 340 and 380 nm and emission was monitored at 510 nm. Drugs were added following 40 seconds of baseline collection, and the average fluorescence output was converted to average calcium concentration via the Grynkiewicz equation (17).

Two-photon microscopy

A custom multiphoton workstation at the University of Wisconsin Laboratory for Optical and Computational Instrumentation (LOCI, www.loci.wisc.edu) was utilized. All samples were imaged with the same power using a TE300 inverted microscope (Nikon, Tokyo, Japan) equipped with a CFI Plan Fluor 20× (N.A.= 1.2; Nikon) objective lens by using a mode-locked Ti:Sapphire laser (Spectra Physics Mai Tai, Mountain View, CA). An excitation wavelength of 765 nm was used to detect the fluorescence signal using a H7422P GaAsP photon counting PMT (Hamamatsu, Hamamatsu City, Japan). Cells were incubated at 37°C using a stage incubator. Images of 1024 × 1024 pixels were acquired using WiscScan (http://www.loci.wisc.edu/wiscscan/) under identical conditions and laser power.

Animal studies

Twenty-one 5 to 6 week-old female athymic nu/nu mice were each given a dorsal subcutaneous injection of SK-N-AS neuroblastoma cells (3×10^6) suspended in 500 μl of 1:1 culture medium and basement membrane matrix suspension (BD Matrigel; Fisher Scientific, Pittsburgh, PA, USA). Tumors were allowed to grow for 4 days before the randomization of the animals into 4 groups of 5 animals each. Tumors were allowed to grow to approximately 200 mm^3 before starting administration of 5 injections of 200 μl R-P104 (approximately 5mg Res per injection) or vehicle over a period of two weeks either in the tissue adjacent to the tumor (peri-tumor) or into the tumor (intra-tumor). Tumor volume was measured twice a week in three dimensions with calipers and the volume was approximated by multiplying the three measurements. On the day after the last dose, the animals were euthanized, photographed, their tumors were harvested, measured in three dimensions using calipers, fixed in 10% neutral buffered formalin and processed for histology. Five-micrometer sections were cut in a masked fashion to obtain sections that encompassed the full circumference of the tumor that were then stained with Hematoxylin-Eosin (H&E). These were examined microscopically and the histopathologic features were recorded as previously described (18-20). Histopathology and tumor section evaluations were carried out independently by two trained observers (DMA and PvG). The percent of the tumor that was necrotic (percent necrotic area) in R-P104- and vehicle-treated tumors was determined in H&E stained tumor sections. The outline of the tumor in each section was traced from a microscopically digitized image, and the areas of viable and non-viable appearing tumor were measured using ImageJ software (Wayne Rasband, NIH, rsbweb freeware).

Statistical analysis

All data were analyzed using one-way ANOVA. If this initial analysis found a significant difference among the groups, then t tests were used to test for pairwise differences between groups. All responses were transformed to the log scale to obtain data, which satisfy the assumptions required for ANOVA. Means and standard errors (SE) were calculated by transforming back from the log scale. Differences were considered significant at $P < 0.05$.

Bioavailability – serum measurements

SKNAS cells were implanted in the flanks of nude mice as described in the animal studies, and tumors were allowed to grow to >200mm^3. A single dose of 5mg R-P104 was administered to three mice each by oral gavage or by peri-tumor or intra-tumor injection. Blood was extracted from the axillary vessels at 30 minutes after drug administration before the mice were euthanized. Serum and tumors were collected and HPLC measurements were carried out using standard procedures (5). Briefly, samples from each mouse were divided into two equal parts. One part was used to measure the concentration of unmetabolized Res. The other part was treated with 10,000 U/mL beta-glucuronidase (Type IX-A, *E.Coli*, Sigma) and 50μl sulfatase (Type VI, *Aerobacter aerogenes*, Sigma) to determine the total concentration of Res (metabolized and unmetabolized). All samples were then incubated at 37°C for 5 hours and extracted with 2 × 0.5 mL ethyl acetate. Upper phases were mixed and the solvent was evaporated. The residual pellets were dissolved in 0.05 mL HPLC solvent B. These samples were then analyzed by the HPLC method to quantify Res concentrations in the serum samples. As an additional control, Res-spiked serum was analyzed and found to be extracted with 90% efficiency.

HPLC method

Samples were analyzed by reverse-phase HPLC using a Gemini C6-phenyl column (4.5 × 250 mm) with 5 micron particle size (Phenomenex, Torrance, CA). The mobile phase consisted of a 40:60 mixture of solvent A (0.1% trifluoroacetic acid in water) and solvent B

(90% Acetonitrile/10% water/0.09%/trifluoroacetic) pumped at 1 ml/min. The eluent was monitored at 305 nm. Calibration curves were obtained using resveratrol standard solutions (0-2000 pmoles) and found to be linear with a correlation coefficient greater than 0.99.

Synthesis of resveratrol metabolites

Preparations of 3-O and 4prime;-O-glucuronidated Res derivatives (3-OGR and 4′-OGR) could be readily accomplished utilizing the synthetic sequences shown in Schematics A and B. Crude products were further purified using a preparative Gemini C6 phenyl HPLC column (Phenomenex, 5μm, 105A°, 250 × 10mm). A gradient program was set starting with 50% mix of solvents A and B linearly increasing to 60%B at 3min, 65%B at 10min, 100%B at 15min, 50%B at 17min. At a flow rate of 3mL/min, the main fraction for the 4′-OGR eluted at 4min, the 3-OGR at 5 minutes and Res at 7min. Purification yielded desired products of ~90% purity. Res 3-O-sulfate (monosulf-Res) and the combination of Res 3-O-4′-O-disulfate and 3-O-5-O-disulfate (disulf-Res) were synthesized according to published procedures (21).

Results and Discussion

Resveratrol metabolites effect on neuroblastoma cell viability *in vitro*

Within minutes after ingestion, Res is predominantly recovered in the serum as sulfated and/or glucuronidated metabolites. The role of these metabolites in the anti-cancer effect of Res is not well understood. Therefore, we initially treated neuroblastoma cells with 100 μM Res or 100 and 200 μM of 3- and 4′-Glu-Res as well as mono- and disulf-Res for 4 days and then normalized their responses to DMSO controls (Figure 1). Unmodified Res reduces the number of viable cells by ~85%. However, the metabolites even at considerably higher concentrations have no effect on viability, indicating that the metabolites do not induce tumor cell death or prevent their proliferation *in vitro*. These findings are consistent with another report that mono- and disulf-Res have considerably lower potency compared to resveratrol in determining the viability of breast cancer cells (22).

Resveratrol uptake

Direct binding targets contributing to the anti-cancer properties of Res are yet to be definitively identified. One obstacle to finding sentinel binding targets for Res is the uncertainty of whether or not Res enters tumor cells. Res is a weak fluorophore with an excitation maximum at 320 nm and emission at 390 nm. In the findings reported here, Res fluorescence was utilized in multiphoton microscopy (23) to observe the cellular localization of Res in neuroblastoma cells. Multiphoton microscopy has the ability to detect weak signals at low wavelengths (broad tunability down to 765 for Res and 780 for optimized auto-fluorescence) without significant photobleaching or cytotoxicity. Figure 2A shows representative optically sectioned slices of cells treated with Res. These images indicate that Res enters and then permeates throughout the cell. Low background auto-fluorescence attributed to NADH is visible at 765 nm (Figure 2B, i) but within 90 seconds of adding Res, the cells become brightly fluorescent (Figure 2B, ii). This suggests that the rate of accumulation of Res is quite rapid at 37°C as is the rate of depletion when Res is removed from the extracellular milieu (Figure 2B, iii). The process is shown to be reversible when the cells again fluoresce on re-addition of Res (Figure 2B, iv). Given the current configuration of the multiphoton microscope, 90 seconds following the addition of Res is the earliest time point that can be taken. At this time Res is observed throughout the cytosol indicating that Res is taken up within this period of time and likely much faster. Res washes out in a similar time frame, indicating that cellular uptake of Res is reversible.

The glucuronidated and sulfated metabolites of Res have fluorescence spectra similar to that of Res with comparable fluorescence intensity. However, when the metabolites were added to the tumor cells (Figure 2C) there was no observable change in cellular fluorescence. This suggests that the uptake mechanism of the metabolites (if any) in tumor cells is quite different from that of Res.

These data indicate that resveratrol and not its metabolites enter neuroblastoma cells and that metabolites are unlikely to contribute to the subsequent intracellular events shown below. It may be possible that in other cell types resveratrol is converted within cells to metabolites that may then activate anti-cancer events (24). However, when SK-NA-S cells were incubated with resveratrol for 0.5-72 hours no metabolites could be detected in either the media or cell extracts (data not shown). Therefore, the studies presented here demonstrate that unmodified resveratrol is needed for transport into tumor cells, and that the unmodified compound is likely responsible for the activation of subsequent intracellular events leading to tumor cell death.

Resveratrol-induced calcium flux

Res has been shown to induce apoptosis in a variety of cancers cell lines. While many potential targets have been evaluated, Res' mechanism of action remains unclear. A rise in $[Ca^{2+}]_i$ has been shown as an early event in apoptotic pathways. A previous study in breast cancer shows that Res induces a rise in $[Ca^{2+}]_i$ that activates the intrinsic mitochondrial apoptotic pathway leading to the activation of caspases and calpain and ultimately to tumor cell death (12). To determine whether Res metabolites induce a calcium response in tumor cells, neuroblastoma cells were loaded with the ratiometric calcium indicator fura-2. Addition of Res (Figure 3) caused an increase in fluorescence reflecting the rise in $[Ca^{2+}]_i$. The change in fura-2 fluorescence could be suppressed when the cells were co-loaded with the calcium chelator BAPTA-AM suggesting that resveratrol-induced changes to fura-2 fluorescence correlates with changes in intracellular calcium levels (data not shown). As seen in Figures 3A and B, none of the Res metabolites evoked a fura-2 fluorescence change indicating that the metabolites did not activate calcium release. Combined with the lack of observable cell death in the tumor cells as described earlier, it would appear that the metabolites are incapable of activating the intrinsic mitochondrial apoptotic pathway *in vitro*.

These *in vitro* studies comparing Res with its glucuronidated and sulfated metabolites suggest that metabolism results in decreased cellular uptake and a corresponding lack of activation of the pathways critical to the anti-cancer activity of Res. Therefore improved efficacy of Res as an anti-cancer drug would depend on the availability of higher levels of free (unmetabolized) Res and lower levels of the metabolites in the tumor environment.

Bioavailability of Res

Res is typically administered in an “oil-based” vehicle in oral efficacy studies in animal models of different types of cancer (25). We have determined that even at doses of 50mg/kg in such vehicles, the serum levels of free Res is less than 1 μM (0.5 μM typically) and tumors are associated with 0.001 μmoles/g Res at peak accumulation. The combined metabolites in the serum are ten to twenty-fold higher (25μM) in concentration than free Res under these conditions. In order to achieve higher levels of Res relative to the metabolites, a water-soluble formulation of Res using a block copolymer was prepared. This formulation allowed us to compare the bioavailability of Res at higher doses (250mg/kg) administered orally, injected next to the tumor (peri-tumor) or directly into the tumor (intra-tumor). The levels of Res in the serum and tumor were determined after a single dose. Using the formulation, free Res levels in the serum increased to >10μM for all three delivery routes

(Table 1) with ten-fold lower metabolite concentrations in the peri- and intra-tumor injections (20 and 34 μM, respectively) than oral delivery (325μM). Oral delivery also resulted in 87% of the Res associated with the tumor being comprised of metabolites and only 0.007μmoles/g of free Res. As anticipated, direct injections resulted in much higher concentrations of Res associated with the tumor. Peri-tumor injections resulted in free Res amounts of 6 μmoles/g and a lower percentage of metabolites (50%). Intra-tumor injections provided the best results with 11 μmoles/g of free Res associated with the tumor and only 15% of the Res in the metabolized forms.

As proof of principle that elevated levels of free Res rather than the metabolites are necessary to achieve a potent anti-tumor effect, peri-tumor and intra-tumor injections of 250mg/kg Res in the water-soluble formulation were tested using a neuroblastoma xenograft mouse model.

In vivo efficacy

First, to test whether tumor inhibition can be achieved with injections of Res, we conducted the experiment using SK-N-AS cells in athymic mice. Tumors were allowed to grow to an approximate volume of 200 mm^3 before starting a series of 5 peri- or intra-tumor injections, each of 200μL R-P104 (approx. 5.0 mg Res per injection) or vehicle over two weeks. Mean tumor size in each group over the course of the study was plotted (Fig 4A) to compare the rate of growth of the tumors in the two groups. In the peri-tumor injected mice, Res treatment showed tumor inhibition of about 88% compared to vehicle-treated controls (P = 0.003). The average tumor volumes of the treated group after 5 doses of R-P104 was 145.8 mm^3 (SE = 54.13 mm^3) while the tumors in the control group grew to an average volume of 1195.4 mm^3 (SE = 506 mm^3). Intra-tumor injections resulted in similar tumor volumes (treated = 177 mm^3; S.E. = 46 mm^3; control = 612 mm^3; S.E. = 46 mm^3; p-value = 0.0036). Next, tumor sections were H&E-stained and viable areas (intact cells with large pleomorphic nuclei that stained predominantly with hematoxylin) were measured with ImageJ software. Analysis of the tumor sections from the peri-tumor injected mice revealed that both drug- and vehicle-treated groups of mice contained areas of decomposing cells showing eosinophilic staining (Figure 4B). This appearance is typically associated with rapidly growing tumors that have outstripped their blood supply. However, in addition to the smaller tumor size in the treated group, on average only 35% of the tumor (21 to 49%) appeared viable compared to 68% (60 to 73%) in the vehicle treated controls, indicating that there was increased cell death related to treatment. Microscopic evaluation showed areas of apoptotic cells with pyknotic nuclei in the drug-treated tumors.

Tumor sections from the intra-tumor injected group suggested improvement over peri-tumor injections with an even smaller percentage of viable areas in the treated tumors. On average only about 8% (0 to 25%) of the tumor was viable in R-P104 treated tumors compared to 55% (30 to 69%) in the vehicle-treated tumors when viable areas were quantified using ImageJ software on the H&E-stained tumor sections. Microscopic evaluation showed extensive areas of necrosis with ghost cells and liquified cell material interspersed with apoptotic cells with pyknotic nuclei in the drug-treated tumors that are absent in the vehicle-treated tumors. Therefore, even though tumor volume measurements showed inhibition of tumor growth in both the peri-tumor and intra-tumor models, the histopathology evaluation of the residual tumors suggested the potential for tumor regression and increased potency with intra-tumor injections (Figure 4C).

In contrast daily oral administration of Res in mice has been shown to result in sub-micromolar serum levels of Res and elevated levels of metabolites (26). These low concentrations of resveratrol are still able to inhibit tumor growth, most likely by inhibiting cell proliferation or tumor angiogenesis. However, these low levels of resveratrol are

insufficient to activate tumor cell apoptosis, and thus tumor regression is not observed. By solubilizing Res using a block copolymer to enable administration of higher doses (250mg/kg) we were able to establish that direct injection of Res into the tumor resulted in the highest levels of free Res in the serum and the tumor; regression of the tumor was then observed. In a new study resveratrol was delivered by peri-tumor injection in a syngeneic mouse model of neuroblastoma, to cause tumor regression (27). Subsequent immunotherapy then proved to be more effective, resulting in a significant improvement in life expectancy. The achievement of tumor regression observed in both of these studies is potentially important, because neuroblastoma arises primarily in the abdominal region as a consequence of sympathetic innervations of the adrenal gland and, therefore, injections are quite feasible to reduce tumor burden as either a primary or neoadjuvant treatment. In addition, by achieving both higher levels of free Res and significant improvements in tumor cell death, these findings support our *in vitro* data that free Res is more directly responsible for anti-tumor activity.

Acknowledgments

We thank Chue Vang for excellent technical assistance.

This work was supported by grants from the National Institutes of Health, R01CA103653 (ASP), the Retina Research Foundation (ASP is the M.D. Matthews Retina Research Foundation Professor), the Mandelbaum Cancer Therapeutics Initiative (ASP and DMA), the American Institute for Cancer Research (PvG) and the UW Carbone Comprehensive Cancer Center (RPH).

References

1. Jang M, Cai L, Udeani GO, Slowing KV, Thomas CF, Beecher CW, Fong HH, Farnsworth NR, Kinghorn AD, Mehta RG, Moon RC, Pezzuto JM. Cancer chemopreventive activity of resveratrol, a natural product derived from grapes. Science. 1997 Jan 10; 275(5297):218–20. [PubMed: 8985016]
2. Goldsby RE, Matthay KK. Neuroblastoma: evolving therapies for a disease with many faces. Paediatr Drugs. 2004; 6:107–122. [PubMed: 15035651]
3. Park JR, Eggert A, Caron H. Neuroblastoma: biology, prognosis, and treatment. Pediatr Clin North Am. 2008; 55:97–120. x. [PubMed: 18242317]
4. Laverdiere C, Liu Q, Yasui Y, Nathan PC, Gurney JG, Stovall M, Diller LR, Cheung NK, Wolden S, Robison LL, Sklar CA. Long-term outcomes in survivors of neuroblastoma: a report from the Childhood Cancer Survivor Study. J Natl Cancer Inst. 2009; 101:1131–1140. [PubMed: 19648511]
5. van Ginkel PR, Sareen D, Subramanian L, Walker Q, Darjatmoko SR, Lindstrom MJ, Kulkarni A, Albert DM, Polans AS. Resveratrol inhibits tumor growth of human neuroblastoma and mediates apoptosis by directly targeting mitochondria. Clin Cancer Res. 2007; 13:5162–5169. [PubMed: 17785572]
6. Gupta SC, Kannappan R, Reuter S, Kim JH, Aggarwal BB. Chemosensitization of tumors by resveratrol. Ann N Y Acad Sci. 2011; 1215:150–160. [PubMed: 21261654]
7. Wenzel E, Soldo T, Erbersdobler H, Somoza V. Bioactivity and metabolism of trans-resveratrol orally administered to Wistar rats. Mol Nutr Food Res. 2005; 49:482–494. [PubMed: 15779067]
8. Marier JF, Vachon P, Gritsas A, Zhang J, Moreau JP, Ducharme MP. Metabolism and disposition of resveratrol in rats: extent of absorption, glucuronidation, and enterohepatic recirculation evidenced by a linked-rat model. J Pharmacol ExpTher. 2002; 302:369–373.
9. Miksits M, Maier-Salamon A, Aust S, Thalhammer T, Reznicek G, Kunert O, Haslinger E, Szekeres T, Jaeger W. Sulfation of resveratrol in human liver: evidence of a major role for the sulfotransferases SULT1A1 and SULT1E1. Xenobiotica. 2005; 35:1101–1119. [PubMed: 16418064]
10. van de Wetering K, Burkon A, Feddema W, Bot A, de Jonge H, Somoza V, Borst P. Intestinal Breast Cancer Resistance Protein (BCRP)/Bcrp1and Multidrug Resistance Protein 3 (MRP3)/Mrp3 Are Involved in the Pharmacokinetics of Resveratrol. Mol Pharmacol. 2009; 75:876–885. [PubMed: 19114588]

11. Maier-Salamon A, Hagenauer B, Wirth M, Gabor F, Szekeres T, Jager W. Increased transport of resveratrol across monolayers of the human intestinal Caco-2 cells is mediated by inhibition and saturation of metabolites. Pharm Res. 2006; 23:2107–2115. [PubMed: 16952002]
12. Sareen D, Darjatmoko SR, Albert DM, Polans AS. Mitochondria, calcium, and calpain are key mediators of resveratrol-induced apoptosis in breast cancer. Mol Pharmacol. 2007; 72:1466–1475. [PubMed: 17848600]
13. Berridge MJ, Lipp P, Bootman MD. The versatility and universality of calcium signalling. Nat Rev Mol Cell Biol. 2000; 1:11–21. [PubMed: 11413485]
14. Pinton P, Giorgi C, Siviero R, Zecchini E, Rizzuto R. Calcium and apoptosis: ER-mitochondria Ca2+ transfer in the control of apoptosis. Oncogene. 2008; 27:6407–6418. [PubMed: 18955969]
15. Ma X, Tian X, Huang X, Yan F, Qiao D. Resveratrol-induced mitochondrial dysfunction and apoptosis are associated with Ca(2+) and mCICR-mediated MPT activation in HepG2 cells. Mol Cell Biochem. 2007; 302:99–109. [PubMed: 17396234]
16. Guha P, Dey A, Dhyani MV, Sen R, Chatterjee M, Chattopadhyay S, Bandyopadhyay SK. Calpain and caspase orchestrated death signal to accomplish apoptosis induced by resveratrol and its novel analog hydroxystilbene-1 [correction of hydroxstilbene-1] in cancer cells. J Pharmacol Exp Ther. 2010; 334:381–394. [PubMed: 20484155]
17. Grynkiewicz G, Poenie M, Tsien RY. A new generation of Ca2+ indicators with greatly improved fluorescence properties. J Biol Chem. 1985; 260:3440–3450. [PubMed: 3838314]
18. Albert DM, Kumar A, Strugnell SA, Darjatmoko SR, Lokken JM, Lindstrom MJ, Patel S. Effectiveness of vitamin D analogues in treating large tumors and during prolonged use in murine retinoblastoma models. Arch Ophthalmol. 2004; 122:1357–1362. [PubMed: 15364716]
19. Grostern RJ, Bryar PJ, Zimbric ML, Darjatmoko SR, Lissauer BJ, Lindstrom MJ, Lokken JM, Strugnell SA, Albert DM. Toxicity and dose-response studies of 1alpha-hydroxyvitamin D2 in a retinoblastoma xenograft model. Arch Ophthalmol. 2002; 120:607–612. [PubMed: 12003610]
20. Sabet SJ, Darjatmoko SR, Lindstrom MJ, Albert DM. Antineoplastic effect and toxicity of 1,25-dihydroxy-16-ene-23-yne-vitamin D3 in athymic mice with Y-79 human retinoblastoma tumors. Arch Ophthalmol. 1999; 117:365–370. [PubMed: 10088815]
21. Wenzel E, Soldo T, Erbersdobler H, Somoza V. Bioactivity and metabolism of trans-resveratrol orally administered to Wistar rats. Mol Nutr Food Res. 2005; 49:482–494. [PubMed: 15779067]
22. Miksits M, Wlcek K, Svoboda M, Kunert O, Haslinger E, Thalhammer T, Szekeres T, Jager W. Antitumor activity of resveratrol and its sulfated metabolites against human breast cancer cells. Planta Med. 2009; 75:1227–1230. [PubMed: 19350482]
23. Zipfel WR, Williams RM, Webb WW. Nonlinear magic: multiphoton microscopy in the biosciences. Nat Biotech. 2003; 21:1369–1377.
24. Murias M, Miksits M, Aust S, Spatzenegger M, Thalhammer T, Szekeres T, Jaeger W. Metabolism of resveratrol in breast cancer cell lines: impact of sulfotransferase 1A1 expression on cell growth inhibition. Cancer Lett. 2008; 261:172–182. [PubMed: 18082939]
25. van Ginkel PR, Darjatmoko SR, Sareen D, Subramanian L, Bhattacharya S, Lindstrom MJ, Albert DM, Polans AS. Resveratrol inhibits uveal melanoma tumor growth via early mitochondrial dysfunction. Invest Ophthalmol Vis Sci. 2008; 49:1299–1306. [PubMed: 18385041]
26. Asensi M, Medina I, Ortega A, Carretero J, Bano MC, Obrador E, Estrela JM. Inhibition of cancer growth by resveratrol is related to its low bioavailability. Free Radic Biol Med. 2002; 33:387–398. [PubMed: 12126761]
27. Soto BL, Hank JA, Van De Voort TJ, Subramanian L, Polans AS, Rakhmilevich AL, Yang RK, Seo S, Kim K, Reisfeld RA, Gillies SD, Sondel PM. The anti-tumor effect of resveratrol alone or in combination with immunotherapy in a neuroblastoma model. Cancer Immunol Immunother. 2011 Feb 22. Epub.

Abbreviations

Res	Resveratrol
$[Ca^{2+}]_i$	Intracellular calcium concentration

R-P104 Resveratrol P104 formulation

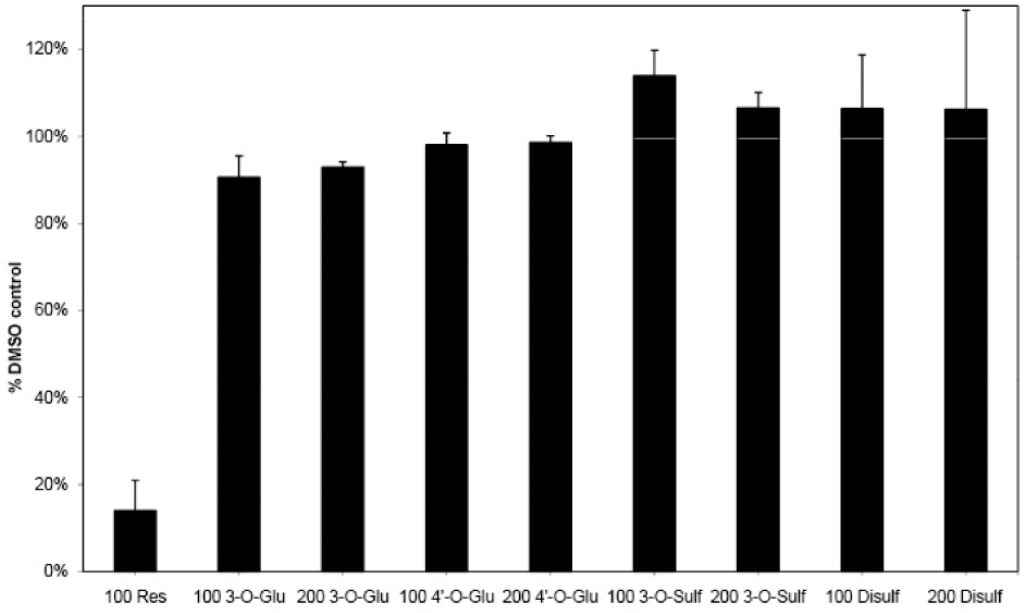

Figure 1.

Viability of neuroblastoma cells treated with Res or the Res metabolites: 3-O- and 4′-O-glucoronidated Res and 3-O- and disulfated-Res. Neuroblastoma cells were treated with 100 μM RES, 100 or 200 μM RES-metabolites for 4 days before viability was measured using Cell Titer Blue. Each experiment was done in triplicates and repeated twice.

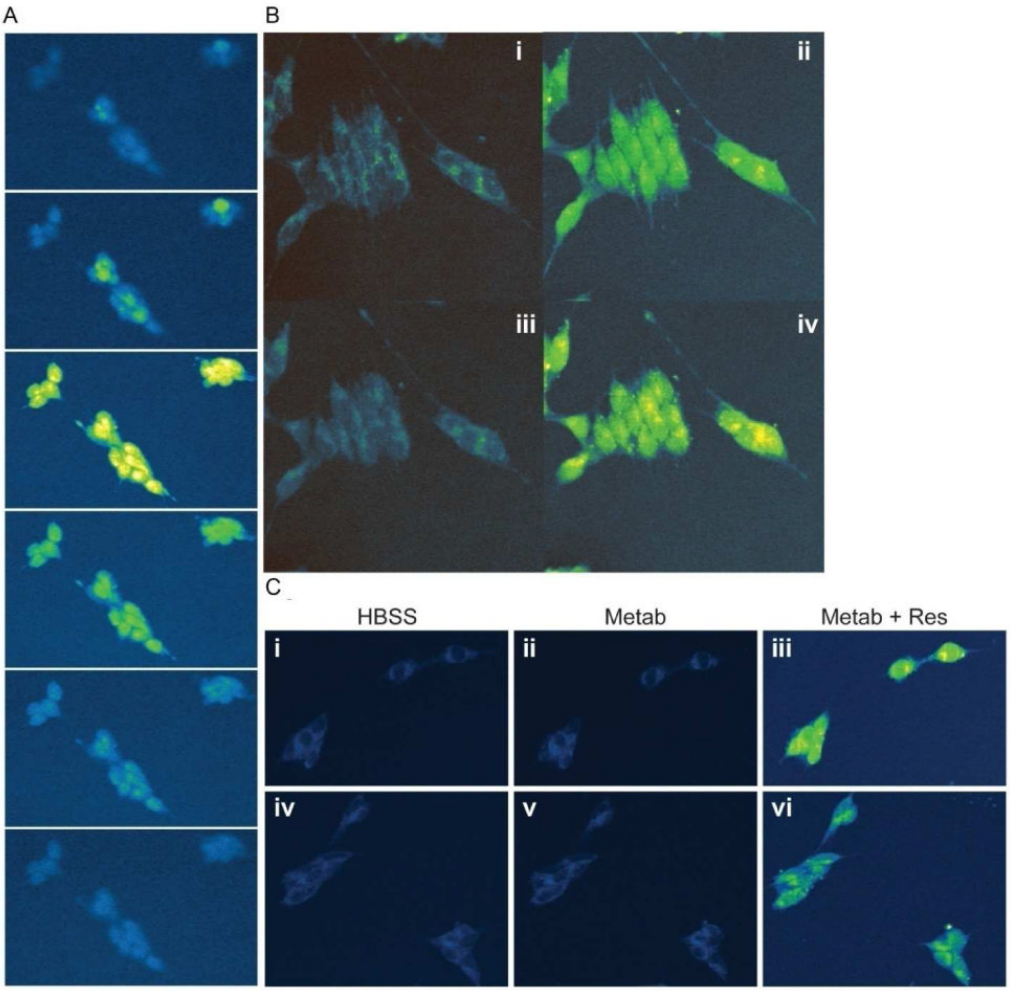

Figure 2.
Res's cellular uptake determined by live-cell multiphoton microscopy excited at 765nm at 37°C. A) Neuroblastoma cells were treated with Res, and subsequently imaged in 2 micron step optical sections. Shown are representative sections through the cells (section numbers 1, 3, 10, 12, 14, and 16). B) i. Cells in Hanks Balanced salt solution (HBSS) were excited at 765nm to show autofluorescence. ii. Similarly imaged 5 minutes following the addition of 100 μM RES. iii. Cells were washed with HBSS to remove Res and imaged again after 5 minutes. iv. Res was re-added to the cells, which leads to an increase in cytoplasmic fluorescence. C) Neuroblastoma cells imaged at 765nm in HBSS (i, iv), with Res metabolites – 100 μM disulf Res (ii), 100 μM gluc-Res (v) and 100 μM Res plus respective metabolites (iii and vi).

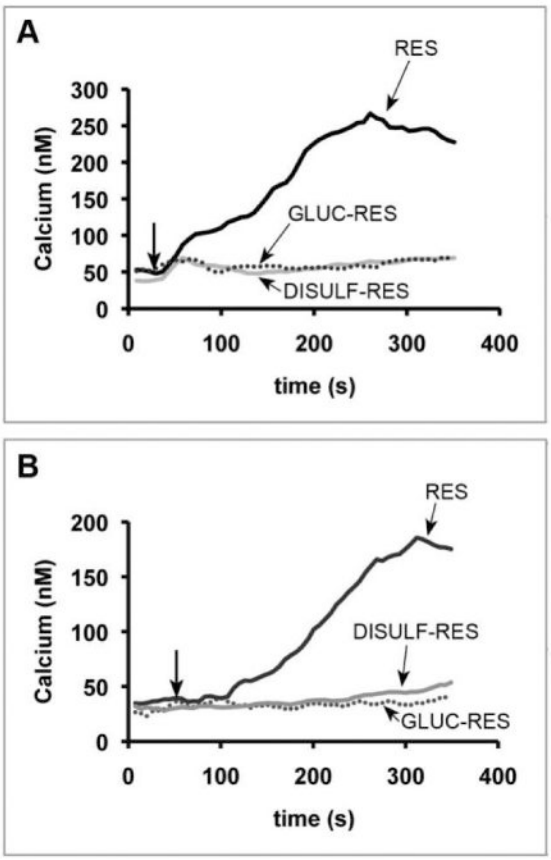

Figure 3.

Res-induced calcium flux in neuroblastoma cells. Neuroblastoma cells, SK-N-AS (A) and NGP (B), were placed on 96 well plates and loaded with fura-2. Live-cell microscopy was used to detect the change in $[Ca^{2+}]_i$. A baseline $[Ca^{2+}]_i$ was established for 40 sec followed by the addition of 100 μM Res (black), 100 μM gluc-Res (dotted), 100 μM disulfated-Res (light gray) as indicated by the arrow. (The same results were obtained with 3-O-sulfated Res).

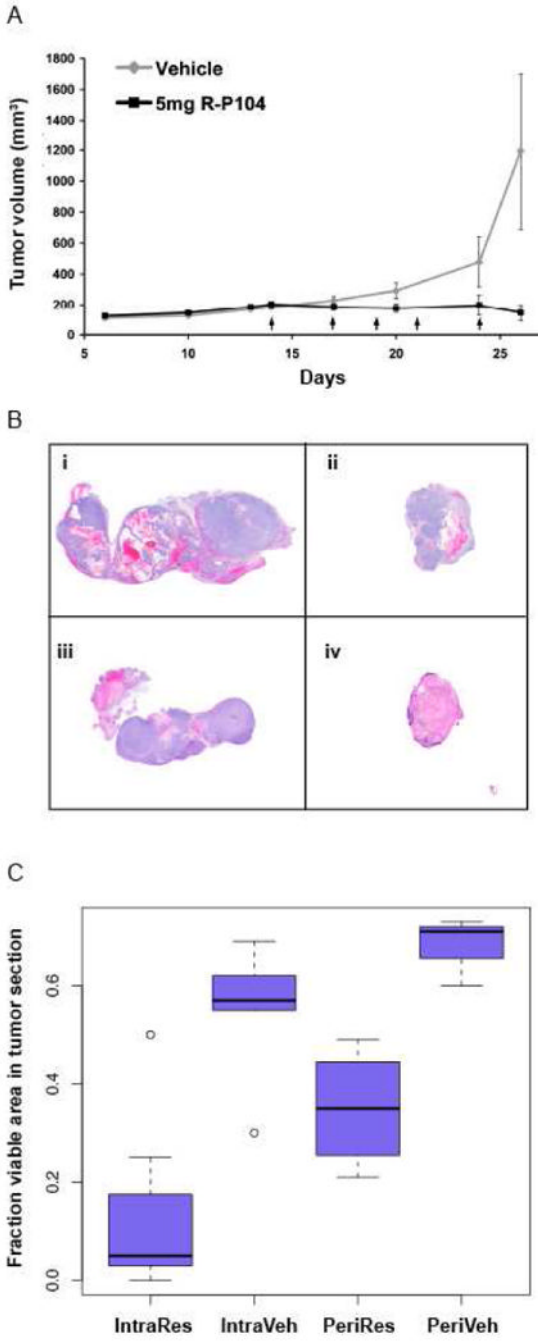

Figure 4.

Res inhibits tumor growth in a xenograft mouse model and induces tumor regression when the concentration of unmetabolized Res in the tumor is increased. A) Tumor growth kinetics during R-P104 treatment course of a SK-N-AS xenograft model by peri-tumor injections. Plotted is the change in average tumor volume in R-P104-treated and vehicle-treated groups of mice. Each arrow indicates a single 200 μL dose. B) Neuroblastoma tumor histology. H&E-stained paraffin sections of tumors removed from mice after five injections of i) vehicle-treated peri-tumor; ii) R-P104-treated peri-tumor; iii) vehicle-treated intra-tumor; iv) R-P104-treated intra-tumor injections. (Hematoxylin stains blue and eosin stains red). C) Plot of average percent viable area in each tumor section from treated and untreated animals.

Three sections from each tumor and five tumors per group were used to calculate the averages.

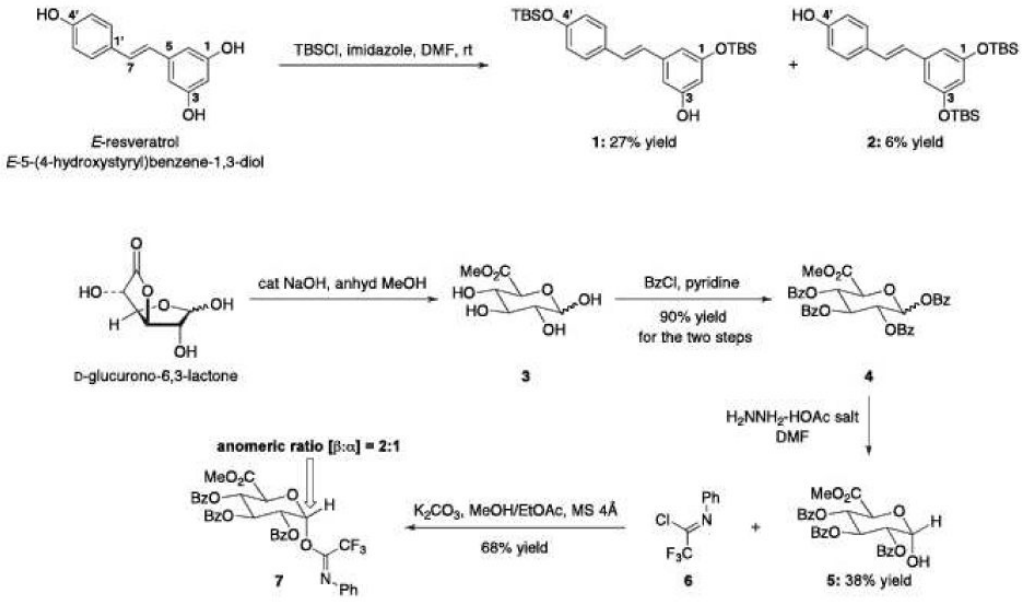

Schematic A.

Chemical syntheses of C3-unprotected Res (**1**), C4′-unprotected Res (**2**), and trifluoromethyl amidate (**7**).

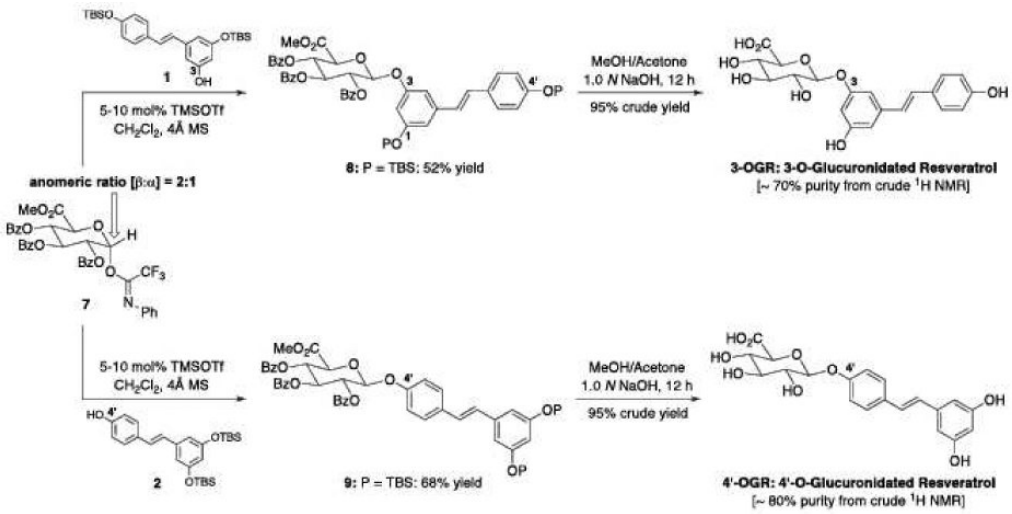

Schematic B.

Chemical syntheses of 3 and 4′ glucuronidated Res derivatives: **3-OGR** and **4′-OGR.**

Table 1

5mg Res-P104 bioavailability after 30mins

	Oral		Peri		Intra	
	Resveratrol	**Metabolites**	**Resveratrol**	**Metabolites**	**Resveratrol**	**Metabolites**
Serum (μM) %	11 3%	325 97%	14 41%	20 59%	13 28%	34 72%
Tumor (μmoles/g) %	0.007 13%	0.046 87%	5.3 45%	6.4 55%	10.9 85%	1.9 15%